Cement and Concrete Composites 125 (2022) 104276

Contents lists available at ScienceDirect

Cement and Concrete Composites

journal homepage: www.elsevier.com/locate/cemconcomp

Effect of calcium stearate and aluminum powder on free and restrained drying shrinkage, crack characteristic and mechanical properties of concrete

Fazel Azarhomayun [a], Mohammad Haji [b], Mahdi Kioumarsi [c,*], Mohammad Shekarchi [a]

[a] School of Civil Engineering, College of Engineering, University of Tehran, Tehran, Iran
[b] Faculty of Civil Engineering, Semnan University, Semnan, Iran
[c] Department of Civil Engineering and Energy Technology at OsloMet - Oslo Metropolitan University, Oslo, Norway

ARTICLE INFO

Keywords:
Concrete
Mechanical properties
Calcium stearate
Aluminum powder
Drying shrinkage
Expander damp proofing

ABSTRACT

Shrinkage is the volume change of concrete without influence of external forces. Drying shrinkage, which occurs after the concrete hardening, is one of the most important causes of the cracking in concrete members. In addition to adverse effects on the appearance of concrete, cracks may reduce the strength and durability by increasing the permeability of concrete and facilitate the entry of aggressive agents into it. Free and restrained drying shrinkage are the most important types of shrinkage. The present study investigated the effect of two admixtures—including damp proofing and expansive materials— on compressive strength, tensile strength, electrical resistivity, modulus of elasticity, unrestrained and restrained shrinkage and water absorption of concrete specimens. In addition, the effect of admixtures on crack properties was investigated. The cracks properties, which occurred in unrestrained shrinkage test, such as average and maximum crack width and total cracks area, were computed by image processing. The results showed that the use of damp proofing additive, (i.e. calcium stearate) reduced maximum free drying shrinkage by 42.4%, maximum restrained drying shrinkage by 22.8%, maximum crack width by 51% and final crack area by 21%. Moreover, the use of expansive additive (i.e. aluminum powder) almost eliminated the free shrinkage, but on average, it increased the restrained drying shrinkage by 18% and reduced the maximum crack width and the final crack area by 2.67 and 27%, respectively.

1. Introduction

Concrete is known as an important building material in structures and infrastructures such as dams, tunnels, bridge decks and buildings. One of the main problems of this type of structures is the creation of many cracks on their surface due to drying shrinkage in concrete. In general, drying shrinkage can be observed in hot and dry areas. The drying shrinkage starts after curing with water [1]. The main cause of drying shrinkage is the evaporation of the water of the capillary pores in hydrated cement paste in an environment with low relative humidity. This phenomenon is related to the evaporation of the water from capillary and gel pores [2]. When the tensile stress, caused by the capillary force in the hydrated cement paste, exceeds the local tensile strength, cracking occurs [3]. Dry surface of concrete layers, reduction of concrete volume and resistance to the volumetric changes of lower layers might cause crack formation in concrete surface. Two methods are recommended for controlling the development of cracks due to drying shrinkage; one of them is to measure water evaporation from concrete surface, and the other is to use proper additives that can prevent cracking [4]. The first method requires monitoring the conditions of curing and controlling the amount of water, whereas the second method needs the use of suitable chemical admixtures, such as shrinkage reduction admixtures, to decrease tensile stresses [5,6]. Using admixtures such as fatty acid-based damp proofing material (DPM), and expansive admixtures can increase the tensile strength of concrete [7]. The use of the DPM reduces the permeability of concrete [8–10]. Besides, according to the ACI 212.3-R16 [11], the DPMs create an impermeable layer along the capillary pores.

The effect of various additives and parameters on drying shrinkage of ordinary concrete has been investigated by many researchers. The effects of different temperature and humidity as well as aggregate size on drying shrinkage were investigated by Refs. [12,13], respectively.

* Corresponding author.
E-mail address: mahdik@oslomet.no (M. Kioumarsi).

https://doi.org/10.1016/j.cemconcomp.2021.104276
Received 17 June 2020; Received in revised form 18 September 2021; Accepted 21 September 2021
Available online 27 September 2021

Table 1
Composition of type II Portland cement.

Composition	CaO	SiO_2	Al_2O_3	Fe_2O_3	MgO	K_2O	Na_2O	C_3S	C_2S	C_3A	C_4AF
%	64.3	21.8	4.5	3.9	1.5	0.54	0.17	56	20	5	12

Fig. 1. Saturated calcuim stearate.

Fig. 2. Aluminum powder which is used in this study.

Table 2
Properties of fine and coarse aggregate, in accordance with the ASTM C33 [43].

Property	Coarse aggregate	Fine aggregate
Specific gravity (saturated surface dry)	2.56	2.55
Water absorption (%)	1.7	2.7
Physical shape	Crushed	Well-rounded

Kioumarsi et al. [14] studied the effect of shrinkage reducing admixture (SRA) on shrinkage of ordinary concrete in different water-cement ratios (w/c) and concluded that using SRA can reduce the free drying shrinkage up to 50%. Collepardi et al. [15] explored the curing impression on shrinkage of concrete containing shrinkage reducing admixture. They resulted that using SRA and CaO-based expansive admixtures was effective in term of shrinkage even in wet curing condition. The effect of expansive admixtures was also investigated by Nagataki and Gem [16]; they observed that these admixtures compensate

Table 3
Type and number of specimens prepared and tested.

Test	Specimen	Dimensions (mm)	Standard
Air content	–	–	ASTM C231
Slump	–	–	ASTM C143
Compressive strength	Cubic	150 × 150 × 150	EN 12390-3
Tensile strength	Cylinder	150 × 300	ASTM C496
Unrestrained drying shrinkage	Prism	75 × 75 × 285	ASTM C157
Electrical resistance	Cubic	100 × 100 × 100	ASSHTO T358
Modulus of elasticity	Cylinder	100 × 200	ASTM C469
Restrained drying shrinkage	Restrained drying Shrinkage	330 ± 3.3 (internal) 406 ± 3 mm (external) 152 ± 6 mm (height)	ASTM C1581
Water absorption	Cubic	750 × 750 × 750	BS 1881-part122

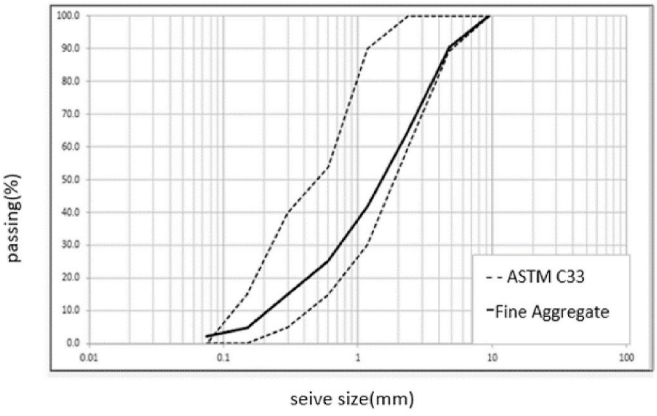

(a)

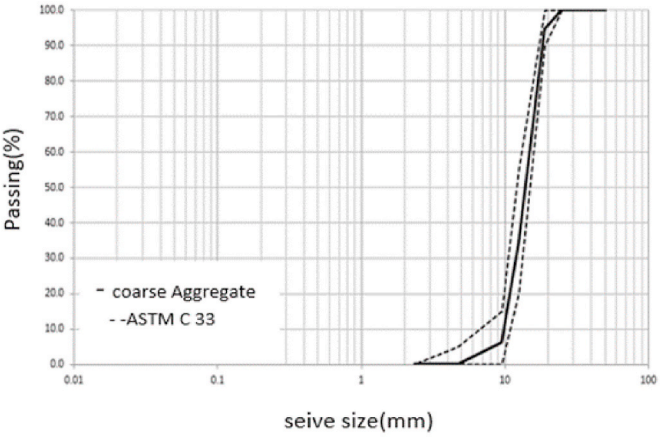

(b)

Fig. 3. Grain size curve for (a) fine aggregate and (b) coarse aggregate.

Table 4
Mixtures proportions.

Group	Mixture ID	Cement (kg/m^3)	Water (kg/m^3)	w/c	Fine aggregate (kg/m^3)	Coarse aggregate (kg/m^3)	[a]EXP % (weight of cement)	Aluminum powder (gr/cm^3)	[b]DPM % (weight of cement)	Calcium stearate (gr/cm^3)	Superplasticizer % (weight of cement)
1	Plain	350	210	0.6	1151	619	–	–	–	–	–
	EXP	350	210	0.6	1151	619	0.0015	1.1	–	–	–
	DPM	350	210	0.6	1151	619	–	–	1	1.08	–
2	Plain	350	175	0.5	1173	632	–	–	–	–	0.5
	EXP	350	175	0.5	1173	632	0.0015	1.1	–	–	0.5
	DPM	350	175	0.5	1173	632	–	–	1	1.08	0.5
3	Plain	350	140	0.4	1196	644	–	–	–	–	0.9
	EXP	350	140	0.4	1196	644	0.0015	1.1	–	–	0.9
	DPM	350	140	0.4	1196	644	–	–	1	1.08	0.9

[a] Expansive admixtures.
[b] Damp proofing material (DPM).

Table 5
The procedure of other experiments.

Experimental tests	Standard	Description
Compressive strength	EN 12390–3 [49]	Compressive strength test was performed on cubic specimens of 150 × 150 × 150 mm in accordance with the EN 12390-3 standard [49] at 28 days of age. The average of the three specimens for each mixture was reported as the compressive strength criterion.
Tensile strength	ASTM C496 [50]	The tensile strength of 30 × 15 cm cylindrical specimens was obtained according to the ASTM C496 [50] at 28 days in which the average of tensile strength was reported for each mixture.
Electrical resistivity	ASSHTO T358 [51]	In order to obtain the electrical resistivity of mixtures, the specimens with the dimensions of 100 × 100 × 100 mm were prepared according to the ASSHTO T358 [51].
Modulus of elasticity	ASTM C469 [52]	Young's modulus test was performed on specimens of 200 × 100 mm according to the ASTM C469 [52] at 28 days
Water absorption	BS1881-part122 [53]	The water absorption test was performed according to the BS 1881-part122 [53]. This test was performed in accordance with the standard on the cores gotten from the 15 × 15 × 15 cm cube specimens. The specimens were stored at 105 °C in the oven for one day. Then, their mass was measured in the dry state as dry weight and the specimens were placed in water for 30 min. After 30 min of immersion of specimens, they were taken out of the water and their mass was measured as wet weight. Then the water absorption was calculated by$((wet\ \ weight - dry\ \ weight)/dry\ \ weight)$

Table 6
Properties of fresh concrete.

Group	Mixture ID	w/c	Slump (cm)	Air content (%)
1	Plain	0.6	21	1.6
	EXP	0.6	22	1.2
	DPM	0.6	19	2
2	Plain	0.5	15	2
	EXP	0.5	17	1.5
	DPM	0.5	13	2.7
3	Plain	0.4	15	2.6
	EXP	0.4	17	2.1
	DPM	0.4	13	3.5

early-age shrinkage. Using MgO-based expansive admixture in low w/c can effectively reduce shrinkage even in dry curing condition [17]. Using type K of expansive agent can decrease drying shrinkage [18]. Wang et al. [19], by examining aluminum powder admixture at doses of 0.013%–0.021% of the cement weight, concluded that this admixture

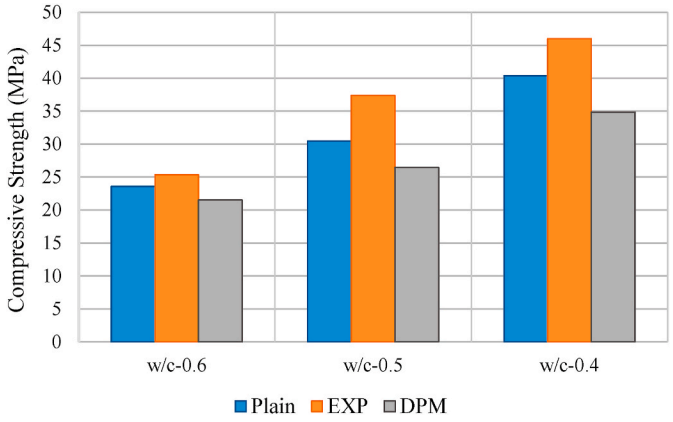

Fig. 4. Compressive strengths at 28 day in specimens with various w/c.

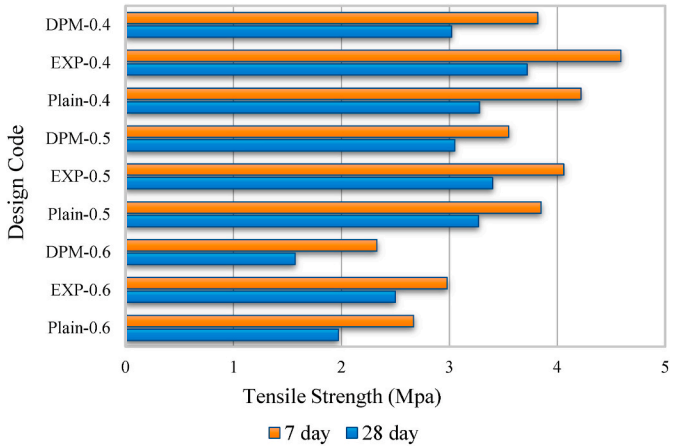

Fig. 5. Tensile strength in specimens with different w/c at 7, 28 day.

compensates early-age shrinkage in concrete. One of the effective measures to compensate the shrinkage, resulted from the expansion caused by hydration of the materials, is to use expansion admixtures of sulfaluminate and CaO-types [16]. Ranjbar et al. [20] investigated the effect of palm oil ash on drying shrinkage and concluded that it could significantly reduce the shrinkage. The same results obtained by Ref. [21]. The effect of slag on drying shrinkage is investigated by Refs. [22,23]. It is reported that slag can significantly reduce the drying shrinkage. However, Wang and Ma [24] compared the effect of fly ash and alkali-activated slag, on drying shrinkage of concrete and concluded that using 30–50% fly ash had better effect on reducing drying shrinkage

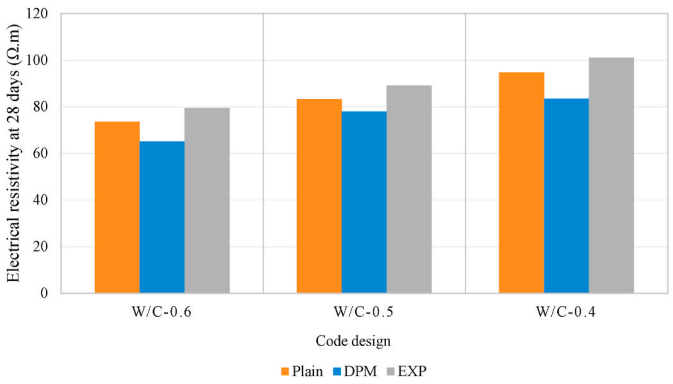

Fig. 6. Electrical resistivity in the specimens at 28 day.

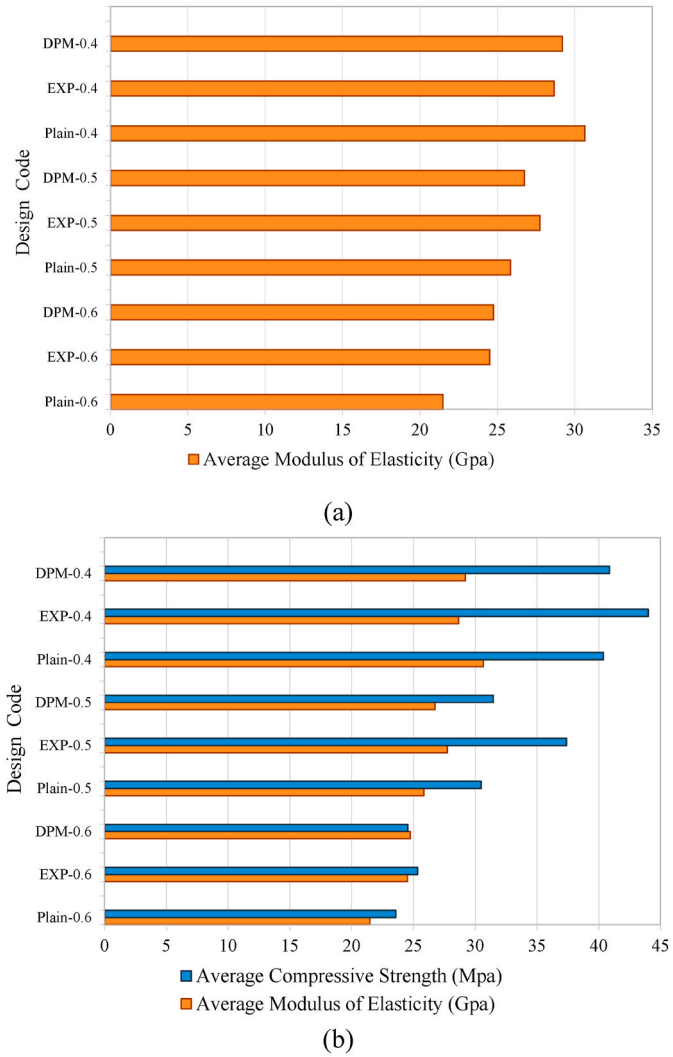

Fig. 7. (a) The amount of modulus of elasticity in specimens and (b) the relationship between compressive strength and elastic modulus.

than slag.

The effect of various additives on the shrinkage of high and ultra-high performance concrete [25–30] and self-compacting concrete [9,31,32] has been widely evaluated by many researchers [12–20]. Recently, nanomaterials and fibers have been used in various fields such as strengthening, improving material properties and etc. [33,34]. The effect of these materials on shrinkage has also been investigated [34–42].

As it is mentioned, drying shrinkage causes cracks; these cracks could be a place for faster penetration of destructive ions into the concrete, which could cause widespread damage. Therefore, minimizing development and size of these cracks by adding additives along with maintaining the mechanical properties of concrete are highly significant. Although there are many investigations dealing with the effect of additives on minimizing the cracks due to drying shrinkage, to the best of authors' knowledge, the effect of calcium stearate and aluminum powder on the free and restrained drying shrinkage of ordinary concretes has not been studied previously. In this study, the effect of these additives, on restrained and unrestrained drying shrinkages and also the characteristics of cracks were investigated, where the results compared with concrete without additives. In addition, the effect of these two additives on mechanical properties of fresh and hardened concrete such as compressive and tensile strength, electrical resistivity, modulus of elasticity and water absorption has also been studied.

2. Methods

2.1. Materials

In the experimental tests, type II Portland cement with a density of 3155 kg/m^3 and a Blaine fitness of 3200 cm^2/g was used. The chemical composition of cement is given in Table 1. Calcium stearate is a white, insoluble powder. Fig. 1 shows the physical form of water-insoluble calcium stearate. In addition, the physical shape of the gray aluminum powder material with the specific gravity of 1.1 is shown in Fig. 2. The composition of the used cement and the properties of the fine and coarse aggregates, which are in accordance with the ASTM C33 [43], are shown in Tables 1 and 2, respectively. It should be noted that the polycarboxylate ether superplasticizer used to regulate performance with the specific gravity of 1.1.

2.2. Specimen preparation

The purpose of this study is to investigate the effect of the admixtures, i.e. calcium stearate and aluminum powder, on drying shrinkage, crack characteristic and mechanical properties of concrete, where three w/c of 0.4, 0.5 and 0.6 were taken into account. The mix design was conducted in accordance with the ASTM C192 [44]. For preparing the specimens, first, the half of sand was poured into the mixer and the rest was mixed with calcium stearate and then added to the mixer. In the specimens containing the aluminum powder, some of the cement was mixed with the admixture separately and then added to the rest of the cement inside the mixer. Then the aggregate was added into the mixer and, subsequently, the cement and water were gradually added to the mixture. Superplasticizer was also mixed with some water from the mix design and then added to the mixture. The resulted paste was kept into the molds for 24 h. All the specimens were placed in lime-saturated water at 23 ± 2 °C. Table 3 shows the geometry and dimensions of specimens and the related used standard for each test. In addition, Fig. 3 indicates the grain size curve of fine and coarse aggregates in accordance with the ASTM C33 [43].

2.3. Mixture proportion

Investigating the effects of calcium stearate and aluminum powder on the properties of fresh and hardened concrete was carried out in nine mixed designs categorized in three groups. Each group was assigned a determined w/c of high, medium or low. The mix designs for all specimens are presented in Table 4. The mix designs were set out to attain a slump value of 15 ± 5. The procedure of the experimental tests performed in this study are provided in Table 5.

Fig. 8. Drying shrinkage test on all specimens of each mix design: (a) DPM-0.5 specimen, (b) Plain-0.4 specimen and (c) EXP-0.6 specimen.

Fig. 9. Putting specimens in the standard condition.

2.4. Experimental procedure

2.4.1. Unrestrained drying shrinkage

Unrestrained drying shrinkage test was performed according to the ASTM C157 [45] standard, in which, the specimens were stored in a chamber with a relative humidity of 50 ± 5 and in the temperature of 23 ± 2 °C [46]. The shrinkage test was performed on the specimens with dimensions of 28.5 × 7.5 × 7.5 cm. The length of the specimens was read after opening the mold, and then the specimens were stored in a room with a temperature of 23 ± 2 °C and a relative humidity of 50 ± 5%. The change in the length of the specimens at regular intervals was displayed by a measuring device. The gauge of the device was 0.001 mm. The purpose of the test is to determine the changes in the length of the concrete that are a sign of shrinkage. In this study, three specimens were prepared for each mixing design. Before making concrete, all the constituent elements had to reached a temperature of 18–24 °C. After making the concrete, the molds were filled in two layers. After 24 h, the specimens were opened from the mold and transferred into the limestone pools. The specimens were immersed in lime water for 24 h and after drying their surface, the first reading related to the change in length was recorded. The specimens were placed in a room with a temperature of 23 ± 2 °C and a humidity of 50 ± 4%. Readings were performed at intervals of 1, 4, 7, 14, 28 days and 8, 16, 32 and 64 weeks. Changes in specimens length were obtained using this equation (1).

$$\Delta Lx = \frac{\text{Initial reading} - \text{Desired time reading}}{G} \quad (1)$$

where G is the length of the gauge and equal to 250 mm and ΔLx is the change in the length of the specimen at the desired time relative to the initial length of the specimen at the time of mold opening.

2.4.2. Restrained drying shrinkage

According to the ASTM C1581 standard [47], the restrained shrinkage test should be performed on ring specimens. The purpose of the test is to investigate the effect of various admixtures on reducing the rate of drying shrinkage cracking. For this purpose, one specimen containing an admixture and one without the admixture were subjected to drying under the controlled environmental conditions and their cracking rates were compared with each other. According to the [47], for each additive, the test must be repeated 2 times. In this experiment, ring-shaped molds were used, in which two steel pipes with a thickness of 12–13 mm were placed inside each other. The inner and outer diameters of tube were 330.3 + 3 mm and 406 + 3 mm, respectively. The height of both pipes was 152 + 6 mm. According to the [47], the inner tube should be made of steel, but the outer tube can be made of steel, PVC or any other material. After construction of specimens, they were placed in a room with a temperature of 21–25 °C and a relative humidity of 46–54%. The concrete base surface was impregnated with a chemical material called cotinine or paraffin to prevent water from evaporating. As recommended by Ref. [47], the amount of shrinkage was calculated by strain gauges mounted on the inner wall of the ring. Strain gauges were connected to the data logger via wires and recorded the strain in the loop on a regular basis. Strain gauges were located in the middle of the ring height on all four sides of the ring. According to the [47], after 24 h of curing, the outer ring was opened and the reading process began after connecting the wires related to the strain gauges. The interval between readings did not exceed 30 min.

Digital photography and their analyses are used to measure crack

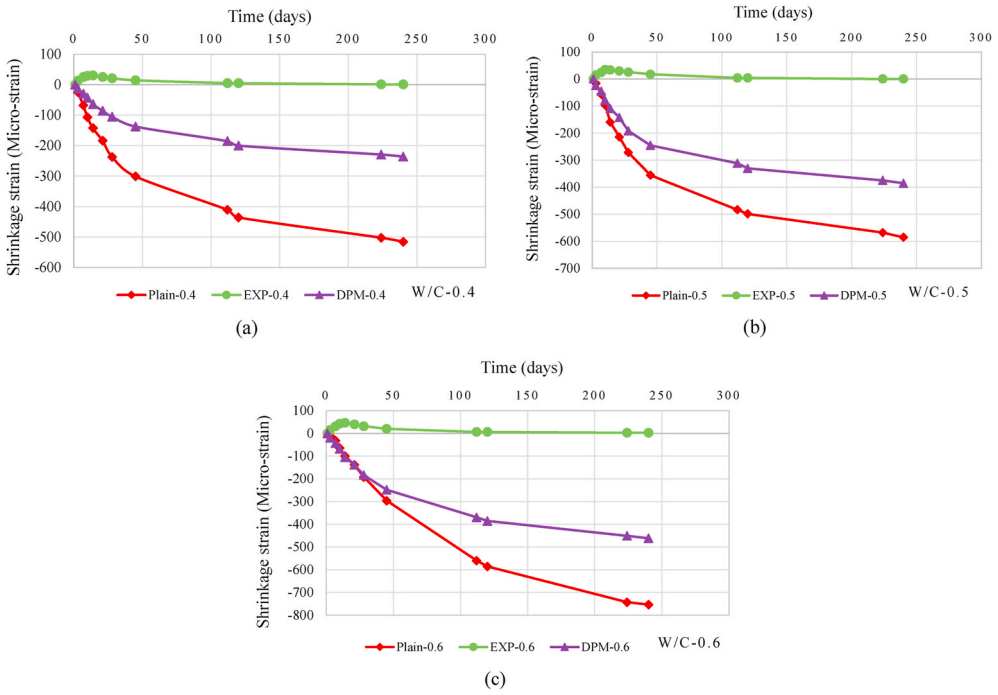

Fig. 10. Free drying shrinkage of the specimens in determined w/c of: (a) 0.4, (b) 0.5 and (c) 0.6.

Fig. 11. Specimens ring test used in restrained drying shrinkage test.

characteristics. Imaging of all the specimens was done at the end of the drying period, i.e. after 30 days. A 12-megapixel camera was used to take the photos, and the distance from the camera to the crack was the same in all specimens. With this process, the cracked surfaces of the specimens were photographed. First, all images were converted from color format to 8-bit gray images. Then, the images were analyzed by code written in the MATLAB software [48]. The developed code, based on the red 8-bit images, requested the user to specify image scale factor and crack border which resulted in creating a binary image of the crack border. In the next step, lines perpendicular to the crack length were drawn at intervals of 10 pixels, and by counting the number of pixels at the intersection of these lines with crack and applying the scale factor, the crack width was calculated. The crack area was also obtained by counting the number of pixels that made up of each crack multiplied by the square of the scale coefficient.

2.4.3. Other tests

In the following table, the description and standard which is used to perform each of the experiment in this study are summarized.

3. Results and discussion

3.1. Fresh concrete

Table 6 provides information on the properties of fresh concrete

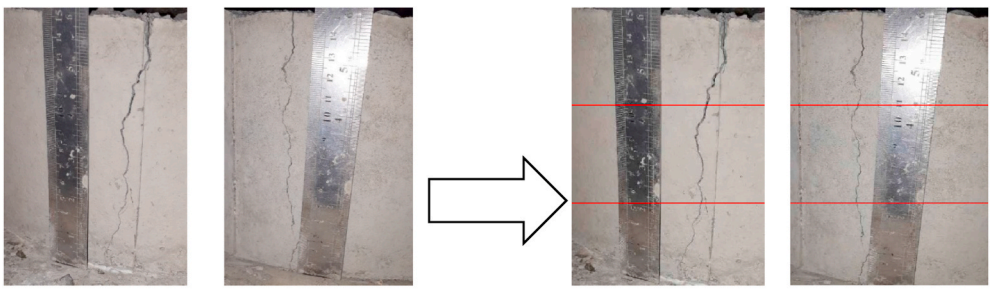

Fig. 12. Crack width in (a) control specimen, (b) specimen containing calcium stearate after 30 days drying, where in (c) and (d) the pictures in parts (a) and (b) are divided into three frames longitudinally.

Fig. 13. Image processing method for FRC in control specimen: (a) gray image as input for processing (b) binary image made from cracked area and (c) cracks width measurement by drawing perpendicular lines to the length of crack.

when the damp proofing material and the expansive admixture were added to the mixture. As can be seen from Table 6, calcium stearate increased the air percentage and reduced the workability of the fresh concrete due to the formation of a hydrophobic layer. In general, it was observed that in all w/c ratios, the difference in slump value between the specimens containing calcium stearate and the control specimens was constant and it can be concluded that changing the value of w/c did not change the effect of calcium stearate on slump compared to the same control specimens. However, the difference in air percentage in specimens containing calcium stearate and the same control sample decreased with increasing w/c ratio. Aluminum powder increased the workability of mortar compared to the control sample as well as concrete containing calcium stearate in all w/c ratios. In addition, it decreased the air percentage due to the increase in volume and filling the porosity through it.

3.2. Compressive strength

Results of the effect of calcium stearate and aluminum powder on compressive strength are provided in Fig. 4. Reaction of calcium stearate with calcium silicate hydrate (C–S–H) produced a wax-like compound which is water-repellent. This material produced less compact, lighter and more stable mixture [54]. In general, the mix designs containing calcium stearate reduced the compressive strength of the concrete. This decrease was higher for the lower w/c ratios. The calcium stearate material had a greater effect on decreasing in the compressive strength. It did not improve gradient porosity of cement paste. Calcium silicate also weakened the bond between cement paste and aggregate as well as interfacial transition zone (ITZ), increased the air percentage and decreased the density [9]. In addition, the mix designs containing aluminum powder increased the compressive strength by increasing in the volume of the concrete and secondary ettringite [9]. As it is shown in Fig. 4, calcium stearate decreased the compressive strength by an average of 11.8% compared to control specimen, while aluminum silicate increased the compressive strength by an average 14.7%.

3.3. Tensile strength

Fig. 5 provides information on the effect of calcium stearate and aluminum powder on tensile strength. Since the tensile strength largely depends on the compressive strength of concrete, the mix designs containing calcium stearate reduced the tensile strength of the concrete, in which the changes of tensile strength were consistent with the obtained results of the compressive strength. Expansive admixture also increased tensile strength at the ages 7 and 28 days. After 28 days, in both admixtures, the greatest effect was observed in the water-cement ratio of 0.6 with an increase of about 12% in tensile strength.

3.4. Electrical resistivity

The effect of calcium stearate and expansive material on electrical resistivity of different mixtures in various w/c ratios is presented in Fig. 6. As shown in this figure, by using calcium stearate and increasing w/c the electrical resistivity decreased (7% reduction compared to control specimen), while by using expansive admixture and decreasing w/c the electrical resistivity increased (10% increment compared to control specimen). Reduction of electrical resistivity can be due to the lower compaction of the material resulting from reaction of calcium stearate with cement, while increasing in electrical resistivity in specimens containing aluminum powder can be due to the increasing of the concrete volume and decreasing of the air percentage.

3.5. Modulus of elasticity

Fig. 7-(a) shows the obtained results of the effect of aluminum powder and calcium stearate on modulus of elasticity of the specimens. Except at the w/c of 0.4, in the other w/c ratios the modulus of elasticity has increased in the DPM and the EXP specimens. The maximum increase in modulus of elasticity occurred in the w/c ratio of 0.6 which was about 14% for the DPM and 15% for the EXP specimens. In Fig. 7-(b), the relationship between compressive strength and elastic are shown. As can be seen from Fig. (7-b), and given that the modulus of elasticity is the ratio of stress to strain, there is almost a correlation between compressive strength and modulus of elasticity.

3.6. Unrestrained drying shrinkage

The unrestrained drying shrinkage test was performed on all the mix designs, as shown in Fig. 8. The length of the prismatic specimens was measured at the ages of 1, 4, 7, 14, 28 days and also 8, 16, 32, 64 weeks. To determine the shrinkage related to each mix design, the specimens were located in the standard condition [45] as shown in Fig. 9. The effects of the calcium stearate and the aluminum powder on the shrinkage of the specimens with different w/c ratios are depicted in Fig. 10. The maximum reduction of drying shrinkage in the plain specimens by adding calcium stearate occurred in w/c of 0.4 by 54% (see Fig. 10a). The reason for this decrease is the permeability of the concrete, caused by water penetration into the capillary pores. The permeability of the concrete is decreased because the combination of calcium stearate with water and cement produces wax-like compounds that are water-repellant [54]. It should be noted that by reducing the w/c ratios, the drying shrinkage of the specimens was decreased. According to Fig. 10, after 240 days, the highest shrinkage strain due to free drying was observed in the plain-0.6 specimens, which was equal to 753 microstrain. Compared to the same control specimen, calcium stearate decreased unrestrained drying shrinkage of specimens up to 39%, 34% and 54% for w/c of 0.4, 0.5 and 0.6, respectively. The trends of strain

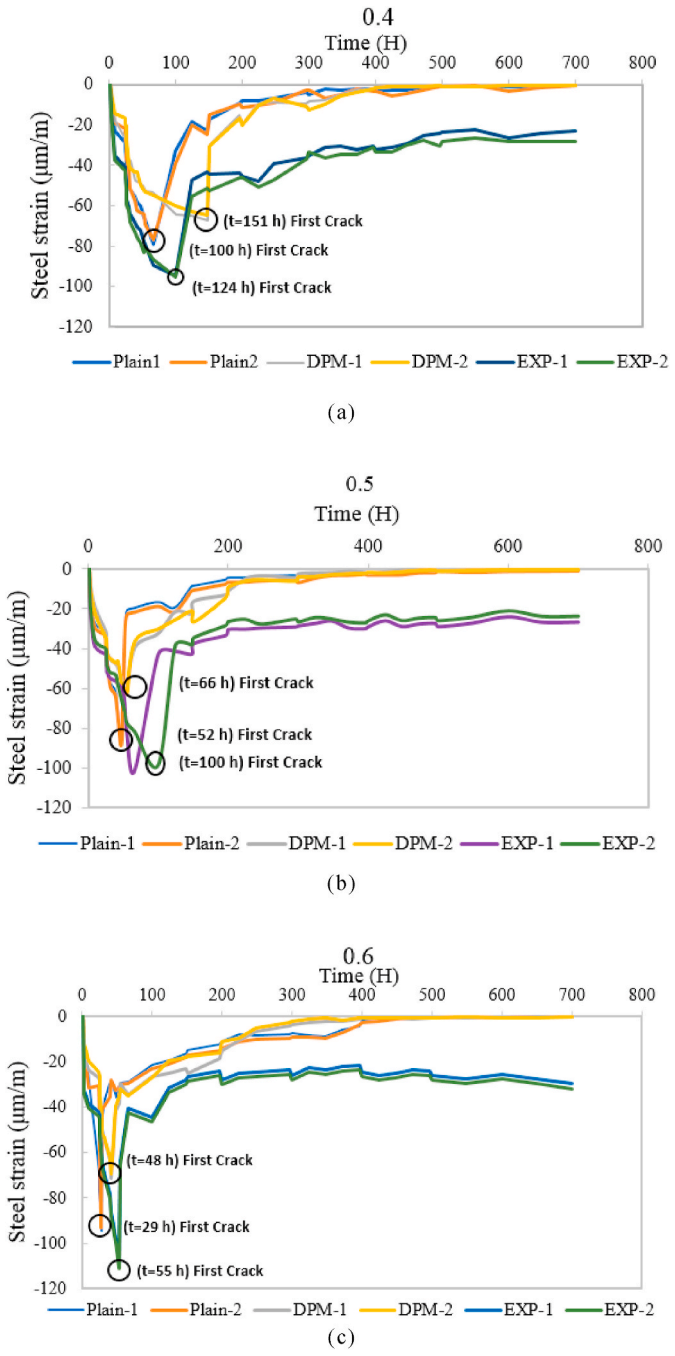

Fig. 14. The steel ring strain-time diagram of mix designs with w/c of (a) 0.4, (b) 0.5, and (c) 0.6.

changes in the plain and the DPM specimens were almost the same, so that at first, the strain diagram increased with a large slope for 120 days and then decreased until it reached to a constant value after 240 days. As shown in Fig. 10, the expansive admixture increased the length of specimens in the early ages (up to 50 days). After that, it reduced the length to a very small extent until the amount of change in length has been almost constant where no noticeable change has been observed until 240 days. It might be due to the significant increase in concrete volume because of secondary ettringite formation. Ettringite can fill larger pores and may essentially lead to a denser and more compact cement paste. Expansive materials significantly increased the amount of calcium hydroxide and crystallization of the concrete.

3.7. Restrained drying shrinkage

The results of this test indicate that approximately one or two wide cracks were seen in the control specimens, whereas in concrete containing admixtures, the cracks were in the form of a few cracks with smaller widths where some of them can be seen as capillary cracks. This was due to the sudden release of stress confined in the concrete. The occurrence of the first crack can be considered corresponding to the strain drop in strain-time curve of specimens. In the control concretes, the stress was released immediately after cracking and the strain amount reached zero. In the concrete containing damp proofing materials and expansive admixtures, the tensile capacity increased, which resulted in higher strength of concrete against internal stresses. Calcium stearate delayed the formation time of first crack compared to the control specimen. In the control specimen with a w/c of 0.4, the maximum strain was equal to 22 microstrain. The maximum strain in the mix design containing calcium stearate was 10 microstrain, which indicates a 54% reduction of the strain compared to the control specimen. The expansive material did not create any crack in the concrete due to the volume expansion. The reason for the expanding of volume is the formation of needle-shaped crystals of eritrengite due to the high porosity caused by their irregular arrangement. Fig. 11 shows the ring specimens that was used to obtain the restrained shrinkage. Fig. 12 indicates different in crack widths in the control specimen and the specimen containing calcium stearate after 30 days drying in the restrained shrinkage test. The pictures in Fig. 12 c and d were divided into three parts. The reason of this division is to change them to gray color (Fig. 13 a) and import them to the software as an input for the image processing. In Fig. 13 b, the gray image was changed to binary image; this image shows the cracks with white color and the rest of concrete area with black color. As shown in Fig. 13 c, the lines were drawn perpendicular to crack length to measure the crack widths in small increments and higher accuracy.

Fig. 14 displays the steel ring strains during the time for different w/c ratios and for concrete specimens without and with calcium stearate and aluminum powder additives. In addition, in this figure the time of occurring first crack on concrete surface for each group is shown. According to the results, for the w/c ratios of 0.5 and 0.6 the longest time of forming the first crack was for the plain, the EXP and the DPM specimens, respectively. However, in the DPM specimens with w/c of 0.4, this

Table 7
Cracks properties in specimens which attained by image processing.

	w/c-0.4			w/c-0.5			w/c-0.6		
Characteristic	Plain	Calcium stearate	Alum. powder	Plain	Calcium stearate	Alum. powder	Plain	Calcium stearate	Alum. powder
Initial cracking time (hour)	100	151	124	52	66	100	29	48	55
Maximum strain (microstrain)	80	68	96	88	64	103	96	72	112
Average crack width (mm)	0.58	0.29	0.14	0.69	0.35	0.22	0.78	0.49	0.33
Maximum crack width (mm)	3.154	1.051	0.761	3.987	2.023	1.271	4.996	3.14	2.114
Total cracks area (mm^2)	60.19	44.37	41.25	73.59	57.96	51.57	91.26	77.39	73.11
Total cracks length (mm)	28.57	34.94	37.65	33.14	39.27	42.56	38.25	44.52	47.83
Average crack width reduction (%)	_	50	75	_	49	68	_	37	57
Total cracks area reduction (%)	_	26	31	_	21	30	_	15	20

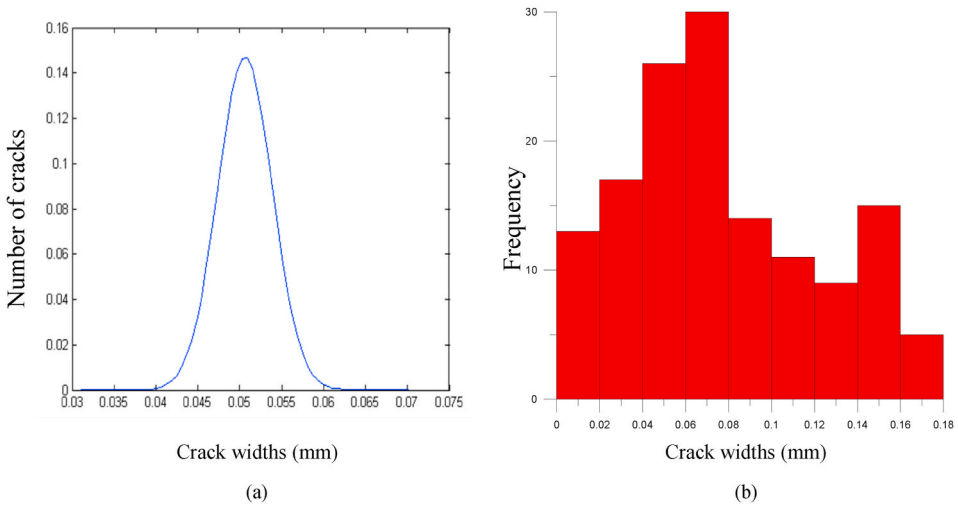

Fig. 15. (a) Crack widths histogram and (b) normal distribution curve of cracks.

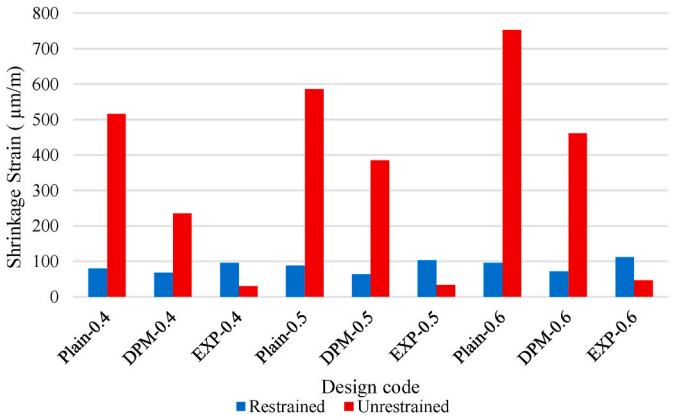

Fig. 16. Maximum unrestrained and restrained drying shrinkage of the Plain, DPM and EXP concrete.

time was larger than other groups which show the better performance of calcium stearate additive than aluminum powder additive in lower water-cement ratio to increase the time of the first crack formation. In general, presented results in Fig. 14 indicate the good performance of aluminum powder and calcium stearate additives in delaying the formation of the first crack in concrete. After the first crack occurred, a sharp decrease in the amount of strain in the steel ring was observed which was due to release of the potential stress in concrete. For the plain and the DPM groups, the strain reached to zero after a sharp drop, while in the EXP group, a residual strain in the specimens at the end of the experiment can be seen. Maximum restrained strain due to the addition of calcium stearate to concrete had the lowest value compared to other specimens, which indicates a good performance of this additive in reducing the strains due to restrained drying shrinkage.

3.8. Image processing

To measure the width of the cracks caused by restrained drying shrinkage, some analyses have been performed using digital photography. Thirty days after drying, using digital camera, imaging was carried out at the specified focal length. By converting from RGB format to BW color mode, the width of the cracks was calculated. After converting the images to BW format, the images were divided into 12 sections and processed with the code written in MATLAB [48,55]. This code creates a binary image of the cracks, which contains information such as crack boundary and scale factor. In addition, lines perpendicular to the length of the cracks were drawn with 10 pixels. Then by calculating the number of points at the intersection of those lines and using the scale factor, the crack widths were calculated. The crack area was measured by multiplying the number of pixels in the forming area and the inverse of the crack scale factor. The characteristics of cracks, which were obtained by image processing, are provided in Table 7.

The histogram of crack widths and its normal distribution are shown in Fig. 15. This figure shows the number and frequency of cracks versus the crack widths. Furthermore, it shows the maximum frequency and number of cracks is for 0.05 mm width. Maximum unrestrained and restrained drying shrinkage of different mix designs are presented in Fig. 16. By increasing w/c ratio, unrestrained drying shrinkage increased for each group. However, no significant changes were seen in restrained drying shrinkage. Calcium stearate and aluminum powder reduced restrained shrinkage; this reduction in the EXP specimens was more than the DPM specimens. In term of free shrinkage calcium stearate reduced the shrinkage. However, aluminum powder increased it in all w/c ratios. The maximum difference between restrained drying shrinkage with free drying shrinkage for the plain and the DPM specimens showed significant reduction of 87% and 84%, respectively. The lower this percentage, the greater the effect of the additive on drying shrinkage was observed. While in the EXP specimens, unlike the plain and the DPM specimens, the free shrinkage values were less than the restrained shrinkage, with difference of 213%. As a result, the performance of aluminum powder on free and restrained drying shrinkage was different, so that it significantly reduced free shrinkage but slightly increased retrained shrinkage.

3.9. Water absorption

The process of water absorption test is illustrated in Fig. 17. Fig. 18 provides information of the effect of calcium stearate and the expansive material on the water absorption of specimens. As shown in Fig. 17, by increasing the immersion time, the water absorption percentage increased. In addition, by increasing w/c ratio, water absorption also increased. The difference in water absorption over time at w/c of 0.4 had the highest value. The highest amount of water absorption occurred in the Plain-0.6 specimen after 24 h, which was equal to 7.35%. In addition, the lowest amount of water absorption occurred in the DPM-0.4 and the EXP-0.4 specimens at the time of 0.5 h, which was equal to 3%. Moreover, due to producing a water repellant layer, the water absorption of the specimens containing the DPM admixture decreased compared to the control specimen. Both additives acted well in reducing water absorption, but in general, the amount of water absorption in the DPM specimens was slightly less than the EXP specimens.

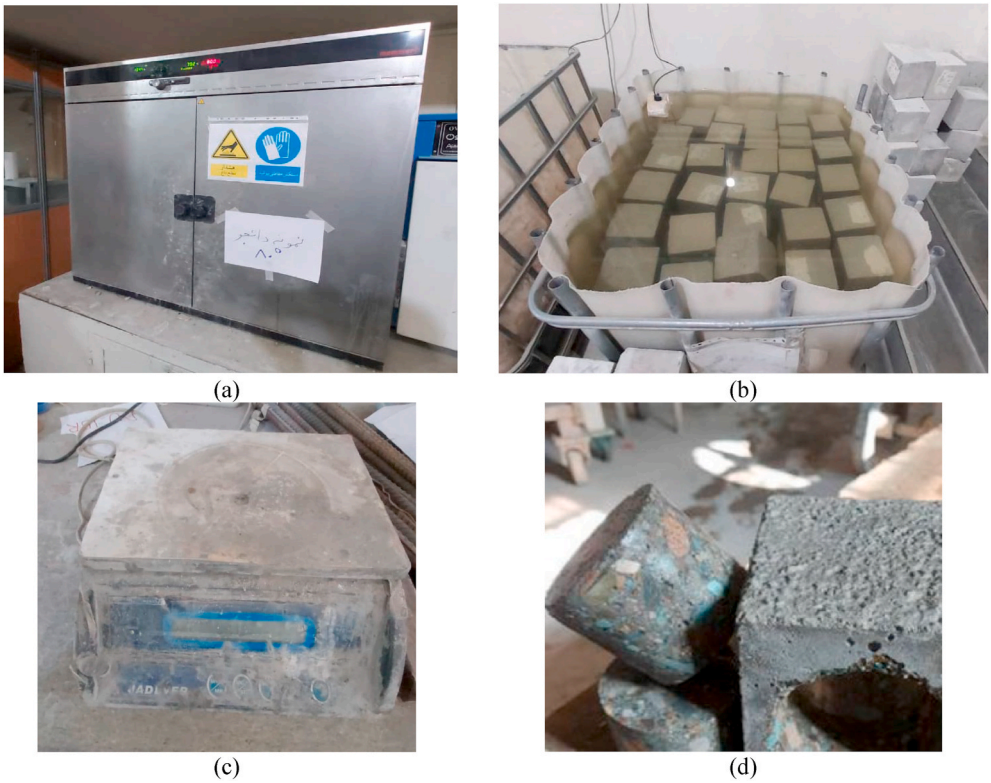

Fig. 17. The process of water absorption test: (a) placing the specimens in oven for one day to measure the dry weight, (b) placing the specimens in water for 30 min to measure the wet weight, (c) wet and dry weight measurement using digital scales and (d) the core extracted from cubic specimen.

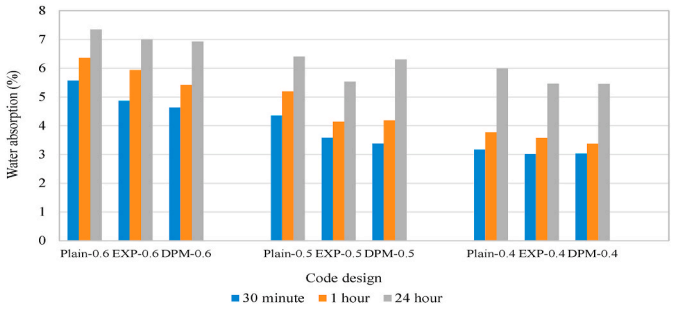

Fig. 18. Comparison of the effect of aluminum powder and calcium stearate on water absorption.

4. Conclusion

In this study, the effects of calcium stearate and aluminum powder on the restrained and unrestrained drying shrinkage of concrete considering three water-cement ratios of 0.4, 0.5 and 0.6 were investigated. Using image processing, the characteristics of cracks caused by restrained drying shrinkage were obtained and examined. Due to the importance of the effect of these additives on other mechanical properties of concrete, the properties of fresh and hardened concrete such as slump, compressive and tensile strength, electrical resistance, modulus of elasticity and water absorption were also examined. The main findings of this study are as follows:

- The largest reduction in the amount of shrinkage strain caused by free drying due to the use of calcium silicate additive occurred in the water-cement ratio of 0.4, which was equal to 54%. The average reduction in free shrinkage due to the use of calcium silicate in all water-cement ratios was 42%. While the use of aluminum powder, due to the formation of secondary ettringite, resulted in filling the large pores and increasing the volume of concrete. Aluminum powder initially increased the volume and length of the sample, then drying shrinkage overcame and reduced the amount of strain to the point that after 120 days the amount of strain reached zero.
- The use of calcium silicate additive not only reduced the strain due to restrained drying shrinkage but also increased the time of the first crack. Using aluminum powder increased the time of the first crack. In addition, it increased the shrinkage strain caused by restrained drying by at least 15% compared to the control specimens. In general, with increasing water-cement ratio, the time to formation of the first crack decreased in all specimens. The highest strain reduction and highest delay in the time of formation of the first crack due to restrained drying shrinkage in comparison to the control specimens occurred in specimens containing calcium silicate which were equal to 28% and 51 h, respectively.
- In general, aluminum powder showed better performance in terms of reducing the cracks characteristics compared to calcium silicate. By applying image processing on restrained drying shrinkage results, it was observed that aluminum powder reduced the total cracks area, average crack width and maximum crack width by an average of 27%, 67% and 67%, respectively, while calcium silicate reduced these parameters by an average of 21%, 45% and 51%.
- The use of calcium silicate reduced workability by an average of 12% and increased the air percentage by an average of 31%. While the use of aluminum powder increased the workability by an average of 10% and reduced air percentage by an average of 23%.
- Calcium silicate reduced the 28-day compressive and tensile strengths because of the formation of a less compact and lighter mixture due to the combination with cement by an average of 12%. However, aluminum powder increased mentioned strengths by an average 15% due to the increasing in volume and producing a more compact mixture, as well as decreasing the mixing air percentage.

- In general, the electrical resistivity decreased with increasing water-cement ratio. Compared to the control specimen, aluminum silicate reduced the electrical resistivity while aluminum powder increased it.
- Increasing water-cement ratio and also test duration caused an increase in water absorption. Water absorption of specimens after 24 h averagely decreased 9% and 5% due to using aluminum powder and calcium silicate, respectively.

In general, and according to the results of this study, it can be concluded that the use of calcium stearate as a damp proofing additive significantly reduces the amount of free and restrained drying shrinkage as well as characteristics of cracks caused by concrete shrinkage. In addition, the use of aluminum powder as an expansive additive has a significant effect on reducing the characteristics of cracks as well as improving the mechanical properties of concrete.

Declaration of competing interest

The authors declare that they have no known competing financial interests or personal relationships that could have appeared to influence the work reported in this paper.

References

[1] Z. Pan, S. Meng, Three-level experimental approach for creep and shrinkage of high-strength high-performance concrete, Eng. Struct. 120 (2016) 23–36, https://doi.org/10.1016/j.engstruct.2016.04.009.

[2] M. Mastali, P. Kinnunen, A. Dalvand, R.M. Firouz, M. Illikainen, Drying shrinkage in alkali-activated binders – a critical review, Construct. Build. Mater. 190 (2018) 533–550, https://doi.org/10.1016/j.conbuildmat.2018.09.125.

[3] P.A.P.C. Aitcin, A. Neville, Integrated view of shrinkage deformation, Concr. Int. 19 (9) (1997) 35–41.

[4] M.C. Garci Juenger, H.M. Jennings, Examining the relationship between the microstructure of calcium silicate hydrate and drying shrinkage of cement pastes, Cement Concr. Res. 32 (2002) 289–296, https://doi.org/10.1016/S0008-8846(01)00673-1.

[5] J. Eid, S. Taibi, J. Marie, M. Hattab, Drying , cracks and shrinkage evolution of a natural silt intended for a new earth building material . Impact of reinforcement, Construct. Build. Mater. 86 (2015) 120–132, https://doi.org/10.1016/j.conbuildmat.2015.03.115.

[6] L. Liu, X. Wang, H. Chen, C. Wan, Microstructure-based modelling of drying shrinkage and microcracking of cement paste at high relative humidity, Construct. Build. Mater. 126 (2016) 410–425, https://doi.org/10.1016/j.conbuildmat.2016.09.066.

[7] S. Monosi, R. Troli, O. Favoni, F. Tittarelli, Cement & Concrete Composites Effect of SRA on the expansive behaviour of mortars based on sulphoaluminate agent, Cement Concr. Compos. 33 (2011) 485–489, https://doi.org/10.1016/j.cemconcomp.2011.01.001.

[8] L. Falchi, U. Müller, P. Fontana, F.C. Izzo, E. Zendri, Influence and effectiveness of water-repellent admixtures on pozzolana – lime mortars for restoration application, Construct. Build. Mater. 49 (2013) 272–280, https://doi.org/10.1016/j.conbuildmat.2013.08.030.

[9] M. Nemati, C. Ramin, N. Mohammad, The impact of calcium stearate on characteristics of concrete, Asian J. Civ. Eng. (2019), https://doi.org/10.1007/s42107-019-00161-x.

[10] A. Lagazzo, S. Vicini, C. Cattaneo, R. Botter, Effect of fatty acid soap on microstructure of lime-cement mortar, Construct. Build. Mater. 116 (2016) 384–390, https://doi.org/10.1016/j.conbuildmat.2016.04.122.

[11] Reported by ACI, committee 212 (Chapter 15): Permeability reducing admixtures, A. 212.3R-10, Report on Chemical Admixtures for Concrete, 2017.

[12] J. Shi, S. Liu, T. Liang, H. Yu, Y. Zhang, Study on shrinkage of ordinary concrete under different temperatures and humidity, 2019, pp. 128–135, https://doi.org/10.1007/978-3-319-95789-0_12.

[13] P. Gao, Y. Chen, H. Huang, Z. Qian, E. Schlangen, J. Wei, Q. Yu, Effect of coarse aggregate size on non-uniform stress/strain and drying-induced microcracking in concrete, Compos. B Eng. 216 (2021) 108880, https://doi.org/10.1016/j.compositesb.2021.108880.

[14] M. Kioumarsi, F. Azarhomayun, M. Haji, M. Shekarchi, Effect of shrinkage reducing admixture on drying shrinkage of concrete with different w/c ratios, Materials 13 (2020) 5721, https://doi.org/10.3390/ma13245721.

[15] M. Collepardi, A. Borsoi, S. Collepardi, J. Jacob, O. Olagot, R. Troli, Effects of shrinkage reducing admixture in shrinkage compensating concrete under non-wet curing conditions 27 (2005) 704–708, https://doi.org/10.1016/j.cemconcomp.2004.09.020.

[16] S. Nagataki, H. Gem, Expansive admixtures (mainly ettringite), Cement Concr. Compos. 20 (1998) 163–170.

[17] L. Mo, M. Deng, A. Wang, Cement & Concrete Composites Effects of MgO-based expansive additive on compensating the shrinkage of cement paste under non-wet curing conditions 34 (2012) 377–383, https://doi.org/10.1016/j.cemconcomp.2011.11.018.

[18] J. Han, D. Jia, P. Yan, Understanding the shrinkage compensating ability of type K expansive agent in concrete, Construct. Build. Mater. 116 (2016) 36–44, https://doi.org/10.1016/j.conbuildmat.2016.04.092.

[19] F. Wang, Æ.Z. Liu, Æ.S. Hu, Early age volume change of cement asphalt mortar in the presence of aluminum powder, Mater. Struct. c (2010) 493–498, https://doi.org/10.1617/s11527-009-9505-z.

[20] N. Ranjbar, A. Behnia, B. Alsubari, P. Moradi Birgani, M.Z. Jumaat, Durability and mechanical properties of self-compacting concrete incorporating palm oil fuel ash, J. Clean. Prod. 112 (2016) 723–730, https://doi.org/10.1016/j.jclepro.2015.07.033.

[21] S. Gao, Z. Wang, W. Wang, H. Qiu, Effect of shrinkage-reducing admixture and expansive agent on mechanical properties and drying shrinkage of Engineered Cementitious Composite (ECC), Construct. Build. Mater. 179 (2018) 172–185, https://doi.org/10.1016/j.conbuildmat.2018.05.203.

[22] H.-J. Kim, M. Tafesse, H.K. Lee, H.-K. Kim, Incorporation of CFBC ash in sodium silicate-activated slag system: modification of microstructures and its effect on shrinkage, Cement Concr. Res. 123 (2019) 105771, https://doi.org/10.1016/j.cemconres.2019.05.016.

[23] M.D. Rubio-Cintas, M.E. Parron-Rubio, F. Perez-Garcia, A. Bettencourt Ribeiro, M. J. Oliveira, Influence of steel slag type on concrete shrinkage, Sustainability 13 (2020) 214, https://doi.org/10.3390/su13010214.

[24] G. Wang, Y. Ma, Drying shrinkage of alkali-activated fly ash/slag blended system, J. Sustain. Cem. Mater. 7 (2018) 203–213, https://doi.org/10.1080/21650373.2018.1471424.

[25] W. Shen, X. Li, G. Gan, L. Cao, C. Li, J. Bai, Experimental investigation on shrinkage and water desorption of the paste in high performance concrete, Construct. Build. Mater. 114 (2016) 618–624, https://doi.org/10.1016/j.conbuildmat.2016.03.183.

[26] Y. Zhang, W. Shen, M. Wu, B. Shen, M. Li, G. Xu, B. Zhang, Q. Ding, X. Chen, Experimental study on the utilization of copper tailing as micronized sand to prepare high performance concrete, Construct. Build. Mater. 244 (2020) 118312, https://doi.org/10.1016/j.conbuildmat.2020.118312.

[27] K. Liu, R. Yu, Z. Shui, X. Li, X. Ling, W. He, S. Yi, S. Wu, Effects of pumice-based porous material on hydration characteristics and persistent shrinkage of ultra-high performance concrete (UHPC), Materials 12 (2018) 11, https://doi.org/10.3390/ma12010011.

[28] H. Yu, X. Zeng, Drying shrinkage and suppression technology of HPC in extremely arid area, KSCE J. Civ. Eng. 23 (2019) 180–190, https://doi.org/10.1007/s12205-017-0626-6.

[29] L. Teng, M. Valipour, K.H. Khayat, Design and performance of low shrinkage UHPC for thin bonded bridge deck overlay, Cement Concr. Compos. 118 (2021) 103953, https://doi.org/10.1016/j.cemconcomp.2021.103953.

[30] Y. Liu, Y. Wei, Effect of calcined bauxite powder or aggregate on the shrinkage properties of UHPC, Cement Concr. Compos. 118 (2021) 103967, https://doi.org/10.1016/j.cemconcomp.2021.103967.

[31] R. Naseroleslami, M. Nemati Chari, The effects of calcium stearate on mechanical and durability aspects of self-consolidating concretes incorporating silica fume/natural zeolite, Construct. Build. Mater. 225 (2019) 384–400, https://doi.org/10.1016/j.conbuildmat.2019.07.144.

[32] R. Pilar, R.A. Schankoski, R.D. Ferron, W.L. Repette, Rheological behavior of low shrinkage very high strength self-compacting concrete, Construct. Build. Mater. 286 (2021) 122838, https://doi.org/10.1016/j.conbuildmat.2021.122838.

[33] M. Haji, H. Naderpour, A. Kheyroddin, Experimental study on influence of proposed FRP-strengthening techniques on RC circular short columns considering different types of damage index, Compos. Struct. 209 (2019), https://doi.org/10.1016/j.compstruct.2018.10.088.

[34] Y. Liu, T. Tafsirojjaman, A.U.R. Dogar, A. Hückler, Shrinkage behavior enhancement of infra-lightweight concrete through FRP grid reinforcement and development of their shrinkage prediction models, Construct. Build. Mater. 258 (2020) 119649, https://doi.org/10.1016/j.conbuildmat.2020.119649.

[35] K.-K. Choi, H. Choi, J.-C. Kim, Shrinkage cracking of amorphous metallic fibre-reinforced concrete, Proc. Inst. Civ. Eng. - Struct. Build. 168 (2015) 287–297, https://doi.org/10.1680/stbu.13.00084.

[36] X.J. Yang, P.M. Wang, S.W. Ming, L.F. Liu, Effects of HEMC powder and PP fiber on the drying shrinkage of cement mortar, Adv. Mater. Res. 1129 (2015) 193–200. https://doi.org/10.4028/www.scientific.net/AMR.1129.193.

[37] K. Zhu, X. Ma, L. Yao, L. Zhao, C. Luo, Effect of polypropylene fiber on the strength and dry cracking of mortar with coal gangue aggregate, Ann. Mater. Sci. Eng. 2021 (2021) 1–7, https://doi.org/10.1155/2021/6667851.

[38] J. Liu, H. Chen, B. Guan, K. Liu, J. Wen, Z. Sun, Influence of mineral nano-fibers on the physical properties of road cement concrete material, Construct. Build. Mater. 190 (2018) 287–293, https://doi.org/10.1016/j.conbuildmat.2018.09.025.

[39] X. Wang, J. He, A.S. Mosallam, C. Li, H. Xin, The effects of fiber length and volume on material properties and crack resistance of basalt fiber reinforced concrete (BFRC), Ann. Mater. Sci. Eng. (2019) 1–17, https://doi.org/10.1155/2019/7520549, 2019.

[40] M. Tafesse, H.-K. Kim, The role of carbon nanotube on hydration kinetics and shrinkage of cement composite, Compos. B Eng. 169 (2019) 55–64, https://doi.org/10.1016/j.compositesb.2019.04.004.

[41] J. Fan, A. Shen, Y. Guo, M. Zhao, X. Yang, X. Wang, Evaluation of the shrinkage and fracture properties of hybrid Fiber-Reinforced SAP modified concrete, Construct. Build. Mater. 256 (2020) 119491, https://doi.org/10.1016/j.conbuildmat.2020.119491.

[42] S.-J. Lee, J.-P. Won, Shrinkage characteristics of structural nano-synthetic fibre-reinforced cementitious composites, Compos. Struct. 157 (2016) 236–243, https://doi.org/10.1016/j.compstruct.2016.09.001.
[43] American Society for Testing and Materials, Standard Specification for Concrete Aggregates, ASTM C33/C33 M-16, 2016.
[44] ASTM C192, Standard Practice for Making and Curing Concrete Test Specimens in the Laboratory, ASTM Int. West Conshohocken, 2006.
[45] ASTM C 157, Standard Test Method for Length Change of Hardened Hydraulic-Cement Mortar and Concrete, 1999.
[46] ASTMC 157/C 157M – 08, Standard Test Method for Length Change of Hardened Hydraulic-Cement Mortar and Concrete C 157/C 157M – 08, 2009, pp. 1–7, i.
[47] C. 1581 Astm, Standard Test Method for Determining Age at Cracking and Induced Tensile Stress Characteristics of Mortar and Concrete under Restrained Shrinkage, 2004.
[48] R.C. Gonzalez, R.E. Woods, S.L. Eddins, Digital Image Processing Using MATLAB, Pearson Education India, 2004.
[49] Bs-En 12390-3, Testing Hardened Concrete- Part3: Compressive Strength of Test Specimens, 2009.
[50] C.C. Test, T. Drilled, Standard Test Method for Splitting Tensile Strength of Cylindrical Concrete Specimens C 496/C 496M, C. Concrete, and B. Statements, 2009.
[51] T.358 Aashto, Standard Method of Test for Surface Resistivity Indication of Concrete's Ability to Resist Chloride Ion Penetration, American Association of State Highway and Transportation Officials, ACI Committee, 2015.
[52] ASTM C 469-94, Test for Static Modulus of Elasticity and Poisson'sRatio of Concrete in Compression, ASTM, USA., 2000.
[53] BS-EN 1881-122, Testing Concrete- Part 122, Method for determination of water absorption, 2011.
[54] A. Maryoto, R. Setijadi, A. Widyaningrum, S. Waluyo, Drying shrinkage of concrete containing calcium stearate, (Ca(C18H35O2)2), with ordinary Portland cement (OPC) as a binder: experimental and modelling studies, Molecules 25 (2020) 4880, https://doi.org/10.3390/molecules25214880.
[55] K. Sathya, D. Sangavi, P. Sridharshini, M. Manobharathi, G. Jayapriya, Improved image based super resolution and concrete crack prediction using pre-trained deep learning models, J. Soft Comput. Civ. Eng. 4 (2020) 40–51, https://doi.org/10.22115/scce.2020.229355.1219.